Plasmons in Pb nanowire arrays on Si(557): Between one and two dimensions

T. Block, C. Tegenkamp, J. Baringhaus, and H. Pfnür
Institut für Festkörperphysik, Leibniz-Universität Hannover, Appelstrasse 2, DE-30167 Hannover, Germany

T. Inaoka
Department of Physics and Earth Sciences, Faculty of Science, University of the Ryukyus, 1 Senbaru, Nishihara, Okinawa 903-0213, Japan
(Received 23 August 2011; revised manuscript received 24 October 2011; published 9 November 2011)

The plasmon dispersion in arrays of nanowires of Pb close to an average Pb coverage of one monolayer was determined on the Si(557) surface using electron energy loss spectroscopy with both high energy and momentum resolution. While we find purely one-dimensional (1D) plasmon losses at a Pb concentration of 1.31 monolayers (ML), measured with respect to the Si(111) surface concentration, the 1.2 and 1.4 ML coverages exhibit wavelength-dependent transitions from 1D to anisotropic 2D properties. However, due to the high anisotropy in the system at all coverages, the dispersion curves exhibit 1D characteristics in both directions. This behavior seems to be related to the Pb-induced refacetting of the Si(557) surface, which depends on Pb coverage. It changes both effective system sizes and coupling strength between miniterraces.

DOI: 10.1103/PhysRevB.84.205402 PACS number(s): 73.20.Mf, 73.21.−b, 79.20.Uv

I. INTRODUCTION

Physical systems at the borderline between one (1D) and two dimensions (2D), which are partly stabilized only by the inevitable coupling to the third dimension, offer a wide variety of new physical phenomena due to their inherent instabilities.[1,2] Electronic correlations play a major role in the physics of low-dimensional systems. They are of fundamental interest since they cause strong deviations from the simple Fermi-liquid behavior.[3] Such systems can be easily realized by the adsorption of submonolayers on anisotropic surfaces of single crystals. A very prominent example is the self-organized formation of atomic chain structures both on isotropic and regularly stepped anisotropic surfaces.[4,5] The intense research on these systems is triggered by the possibility of a comprehensive characterization and selective manipulation of these structures with a variety of techniques.[6–11] Though vicinal substrates allow to grow single domain structures, these high-index surfaces easily undergo refacetting processes, as reported recently, e.g., for Au submonolayer coverages grown on vicinal Si(111) surfaces.[12]

Single metallic chains would be the ultimate limit of size reduction for electric interconnects, but at present, the realization of an atomic wire can be done only by using well established concepts of self-assembly. On the other hand, such systems need not be necessarily metallic. They frequently undergo metal-insulator transitions at low temperature.[13] Therefore the study of electronic transport properties is of high interest, since this method can probe inherent electronic instabilities in these low-dimensional structures directly.[14–16]

On an insulating substrate, the low-energy excitations necessary for electronic transport yield direct information about the electron density and electronic scattering properties within and in-between the wires. An alternative approach to get this information is the excitation of plasmons. According to classical theories,[17] the same electron density should be involved in the formation of these collective density oscillations. However, these high-energy excitations compete with intra- and interband electron-hole pair formation. Thus they yield supplementary information about the electronic system near the Fermi level. In particular, it is an open question whether plasmonic excitations in wire arrays with a 1D Fermi surface exhibit the same dimensionality. Due to their coupling with the electron-hole pair decay channels and short plasmonic lifetimes, effective mixing of 1D and 2D states may be possible. A system like Pb/Si(557), which is studied here, is a good test candidate for this purpose, since it combines 2D with 1D properties, as explained below.

On the other hand, plasmons in low-dimensional systems are interesting study objects by their own. In thin films or nanowires with cross-sectional dimensions of the order of the Fermi wavelength, low-dimensional plasmons are predicted to exist with the plasmon energy vanishing in the long-wavelength limit.[18,31] Their properties are by far not yet fully understood, as obvious from recent investigations of plasmonic properties of graphene layers on the C-face of SiC(0001) and on Ir(111).[19,20] While we were able to identify the close coupling between plasmonic and electron-hole pair excitations resulting in the formation of plexcitons, we found that the slope of plasmon dispersion is almost independent of the position of the Fermi level. Neither can this property be understood by the standard theories of low-dimensional plasmonic exciations nor was the existence of multipole plasmons in these systems predicted by theory.[20]

The Pb/Si(557) system in the monolayer range of Pb concentration is exactly one of these systems illustrating the intruiging borderline between one and two dimensions. As it turns out, this surface orientation in presence of Pb is only stable up to about 1 monolayer (ML) coverage [concentration is measured with respect to the Si(111) surface atom density, with this calibration the physical monolayer extends up to 1.5 ML], but forms facets of various orientations at higher Pb coverages. Particularly, at 1.31 ML Pb coverage, the surface facets are at (223) orientation[21] and a reversible temperature-driven semiconductor-insulator transition in the direction perpendicular to the steps is observed when temperature is lowered below 78 K.[22] Along the steps, however, a semiconductor-metal transition is found,[15,23] leading to quasi-one-dimensional conductance. The transition in the $[\bar{1}\bar{1}2]$ direction was assigned

to nesting and band-gap formation in this direction. While this transport signature depends sensitively on coverage and on the homogeneity of the sample, the formation of (223) facets depends only marginally on the exact coverage.[21,24] From a crystallographic point of view, the Pb-induced formation of (223) facets instead of a (557) orientation provides direct evidence of the pronounced coupling of the wires and of the importance of the electronic structure of the surface states.[25] This is exemplified also by the long-range interaction between Pb decorated step edges,[26] which keeps the Peierls gap open up to a Pb concentration of 1.5 ML in the direction normal to the steps,[27] and by anomalies in the surface magnetoconductive properties around 1.3 ML coverage.[28]

In the study presented here, we concentrate on the high-energy plasmonic excitations in the Pb wire structure close to the Pb monolayer. In particular, we want to address the question to which extent the effective 1D property in conductance, found close to 1.31. ML, can also be seen in the plasmonic excitations. Since the plasmon dispersion is sensitive to the density of electrons in the surface conductance bands and to band curvature, we obtain complementary information even at Pb coverages where the concentration of local defects prevents macroscopic conduction measurements.

II. EXPERIMENTAL SETUP

Our experiments were carried out in a UHV chamber at a base pressure of 5×10^{-11} mbar equipped with a load lock system with a combination of a high-resolution electron-energy loss spectrometer and the deflection unit of a low-energy-electron-diffraction (LEED) system for spot profile analysis (SPA-LEED) for high momentum resolution.[29] The electron source and the detector are fixed in this instrument so that the incident and the specularly reflected beam appear at an angle of 6° with respect to the surface normal. Although spectra of inelastically scattered electrons can be measured in the whole surface Brillouin zone (SBZ), all spectra reported here were taken close to the (00) beam for intensity reasons. With the apertures used here, an energy resolution of about 10 meV can be achieved. While momentum resolution on Si surface can be tuned routinely below 1% SBZ, it depends for adsorbed layers on their quality.

Pb was evaporated out of a ceramic crucible heated by a tungsten filament at pressures not exceeding 3×10^{-10} mbar. A microbalance was used to control the amount of Pb. The monolayer (1 ML = 7.84×10^{14} atoms cm^{-2}) of Pb is given here with respect to the Si(111) surface. For fine tuning, we used the phase diagram for Pb/Si(111) measured in detail by Tringides and co-workers, see, e.g., Ref. 30. In particular, the DS-regime (devil's staircase) was used to determine the coverage within 1% of a monolayer (for further details, see Ref. 21). The Si(557) samples (1×1 cm^2) were mounted on a manipulator, which was cooled by ℓHe. Perfect Si(557) surfaces were prepared by degassing the sample for many hours until the pressure was below 1×10^{-9} Pa at 600 °C. The removal of the oxide was done by heating the sample several times up to 1100 °C. Higher flash temperatures rearrange the metastable (557) surface into large (111) domains separated by step bunches. The high-temperature steps were all performed by electron bombardment from the rear of the sample. Measurements were carried out both with and without He cooling.

III. RESULTS AND DISCUSSION

A. The 1.31 monolayer Pb coverage

We first concentrate on the results close to a Pb concentration of 1.31 ML on the (223)-facetted Si(557) surface. This concentration corresponds to the optimal Pb coverage at which one-dimensional conductance along the miniterraces was found at temperatures below 78 K.[15] A LEED pattern obtained with the SPA-LEED instrument at this Pb concentration and after annealing of the sample at 640 K is shown in the left part of Fig. 1. Along the $[\bar{1}\bar{1}2]$ direction normal to the steps, a much wider spot separation than that expected for the (557) surface is seen, which corresponds to (223)-facet formation. A side view in real space of this regularly stepped facet with a terrace width of $4\frac{2}{3}$ atoms is shown in the top right part of Fig. 1. Pb at the given concentration does not cover the step edges.[26] On each terrace, a mixed phase consisting of $\sqrt{3} \times \sqrt{3}$ and

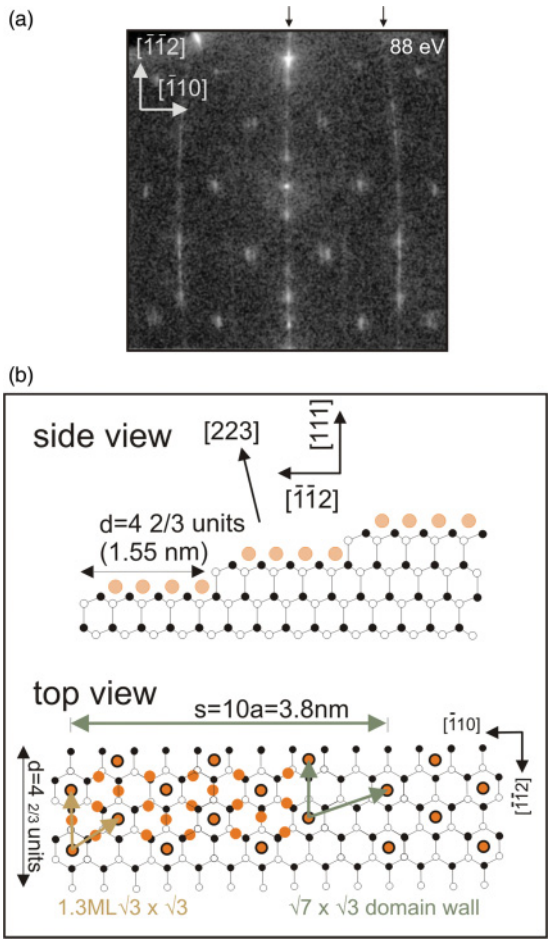

FIG. 1. (Color online) (a) LEED pattern of Pb/Si(557) at 1.31 ML of Pb. Middle row of spots is due to the step train of the (223) facet, right and left rows mark period doubling at step edges. From the splitting of the $\sqrt{3} \times \sqrt{3}$R30° superstructure, the actual Pb coverage is determined. Electron energy is 88 eV. (b) Schematic side view (upper graph) and view from on top of the local structure formed on the (223) facets induced by the Pb coverage.

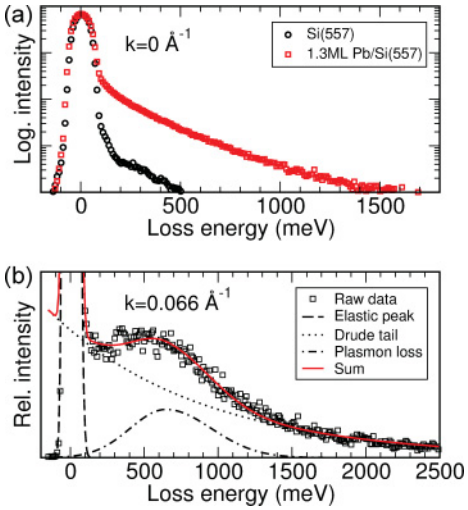

FIG. 2. (Color online) (a) Comparison of electron-energy loss spectra on Si(557) of the clean Si substrate (◯) and with adsorbed 1.31 ML of Pb (□) at $k_{\parallel} = 0$. The conducting nature of the Pb monolayer results in a strongly enhanced inelastic background (Drude tail). (b) Separation of the EELS spectra into elastic (dashed) and inelastic contributions (Drude tail, dotted, and plasmonic loss, dashed dotted). Full line represents the best fit. $E_{\text{elastic}} = 20$ eV.

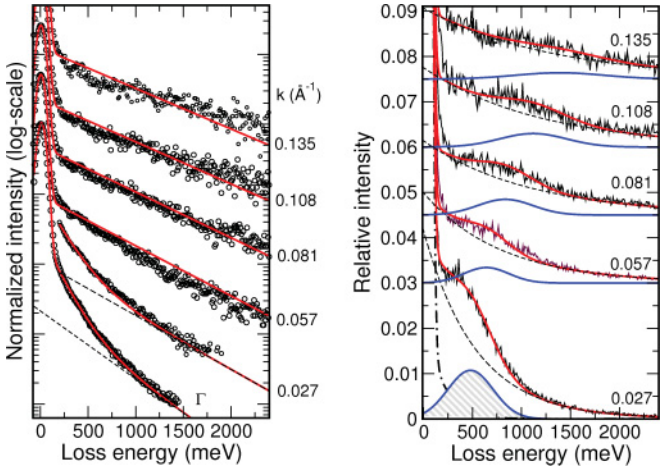

FIG. 3. (Color online) Set of EEL-spectra at a Pb concentration of 1.31 ML as a function of $k_{\parallel}$. Left panel was measured in the direction perpendicular (semilog plot) and the right panel (linear scale) is parallel to step edges. Numbers on the right side of each graph indicate the $k_{\parallel}$ values in Å^{-1}. Dispersion of the plasmonic loss is only seen in the direction parallel to steps. Spectra are normalized to the elastic peak intensity, but were shifted for better visibility.

$\sqrt{3} \times \sqrt{7}$ unit cells is formed with the former being the majority at a Pb concentration of 1.31 ML. The $\sqrt{3} \times \sqrt{7}$ unit cells therefore form domain walls whose concentration depends on Pb coverage. The signature of this domain wall formation is the characteristic spot splitting of the $\sqrt{3} \times \sqrt{3}$ spots seen in Fig. 1. The size of splitting allows fine tuning of Pb concentration, as mentioned.

We carried out sets of k-resolved EELS measurements both in directions parallel and perpendicular to the step direction at room temperature, with ℓN_2 and with ℓHe cooling. In the latter case, temperatures below 40 K were reached, which are clearly below the phase transition between activated two-dimensional conductance at high temperature and 1D metallic conductance below 78 K. Nevertheless, we obtained identical EELS results at all temperatures within error bars. Therefore we will not discriminate between low- and high-temperature data in the following.

At a Pb concentration of 1.31 ML, it is obvious from the EELS spectra shown in Fig. 2 at $k_{\parallel} = 0$, i.e., at the position of the (00) beam, that the system has become metallic. Qualitatively, the same results were obtained in the perpendicular direction. As expected, the low-energy electronic excitations in a 2D metallic system cause a continuum of losses that falls off exponentially as a function of energy, as seen in the semilog plot of Fig. 2. This continuous background is enhanced by more than one order of magnitude in presence of the Pb layer compared to the clean Si(557) surface, indicating that the Pb layer has strongly modified and filled the electronic surface states, in agreement with results from photoemission.[25] Plasmons in 1D or 2D systems go to zero energy in the long-wavelength limit. Therefore no characteristic plasmonic losses are seen in this spectrum. All spectra shown in this paper are normalized to the elastic peak intensity.

These losses, however, are clearly visible when we measured off-specular directions. Sample spectra at various values of $k_{\parallel}$ are shown in Fig. 3 both parallel and perpendicular to the step direction of the Pb coverage of 1.31 ML. This concentration of Pb turned out to be special in the sense that only at this concentration, we were not able to identify characteristic plasmonic losses in the direction perpendicular to the Pb wires, whereas they are clearly visible in the parallel direction. This is quite unexpected, since in both directions the Drude tail is clearly visible, which characterizes the system of being metallic in both directions.

Before we discuss possible physical scenarios for this behavior, we concentrate on a more quantitative analysis of the measured data. For this purpose, positions of inelastic losses, their half-widths (FWHM) and loss intensities were determined using fit procedures for the loss spectra at constant $k_{\parallel}$. The parametrization of the loss spectra is illustrated in Fig. 2(b). The form of the elastic peak was parametrized by Gaussian functions for the uncovered Si(557), and we assumed that the elastic peak form remains unchanged by adsorption. For the Drude tail, we assumed an exponential dependence on loss energy.

From these fits, we determined dispersion curves along and parallel to the wires, i.e., as a function of $k_{\parallel}$ and $k_{\perp}$, respectively. The dispersion parallel to the wires for the Pb concentration of 1.31 ML, shown in Fig. 4. This dispersion is almost linear, which is compatible with a 1D signature of the plasmonic properties on a wire with finite width. In this case, the dispersion is expected to behave like $\omega \propto k_{\parallel} a \sqrt{|\ln(k_{\parallel} a)|}$ for small $k_{\parallel} a$, where $2a$ is the width of the wire.[18,32]

1D band filling and nesting observed for the Pb coverage of 1.31 ML previously[15,25] at first sight seems to be the obvious reason for the observation of a 1D plasmonic loss at this Pb coverage. However, the band gap found was only of the order of 20 meV in the direction normal to the steps, and the excitation of interband plasmons across this small gap

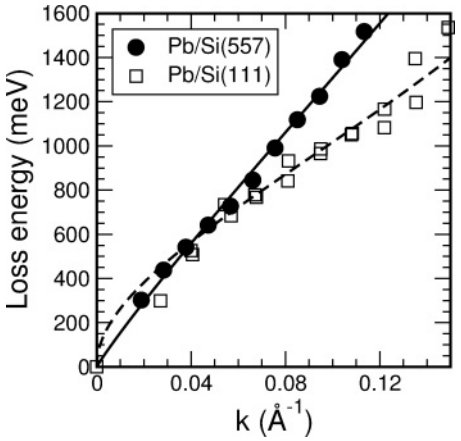

FIG. 4. Dispersion parallel to Pb wires for coverages 1.31 ML (dots) on the (223)-oriented facets of Pb-covered Si(557). For reference, also the dispersion of the high coverage (1.33 ML) $\sqrt{3} \times \sqrt{3}$R30° phase on flat Si(111) is shown (squares). The solid curve corresponds to the 1D fit as described in the text ($m^* = 0.4m_e$ and $N_{1D} = 3.6 \times 10^7$ cm^{-1}). The dashed curve is a 2D fit with the nearly free electron gas (NFEG) model with an effective mass of $0.4m_e$ and an electron density of $N_{2D} = 2.4 \times 10^{14}$cm^{-2}.

should be easily possible, especially since the widths of the plasmonic losses found here are much wider than 20 meV. The Drude tail, measured for loss energies larger than this gap in $k_\perp$ direction, corroborates this expectation, which is in agreement with the temperature independence of our results. We explicitly performed tests at temperatures around 40 and 95 K, i.e., below and above the 1D-2D phase transition found earlier.

Nevertheless, despite optimal ordering of the (223) facets at this Pb concentration, as checked with LEED, the excitation probability for plasmons in the direction normal to the steps must be extremely low or even zero. An obvious explanation of this behavior is that the plasmonic excitations on individual Pb-covered terraces are still be sufficiently decoupled from each other, so that collective excitations in this direction would only be possible as standing waves on individual wires, similar to those found for the $DySi_2$ wires on stepped Si.[33] Higher modes, like those found there on wires that are only 1.55 nm wide, would have excitation energies above 1 eV and would be hard to detect within the small signals measured in this experiment. However, such a simple interpretation has to be taken with caution (see below).

As a first attempt for a more quantitative description, we calculated the dynamical response of a 1D system[34] in a narrow strip,[35] i.e., of a wire with monolayer height and with finite width, and of a 2D system on a plane,[36,37] using the local-field correction theory to take account of the exchange-correlation effects. For the 1D system, we assumed a width of four atomic Si unit cells for the Pb wire, i.e., the width of a miniterrace at 1.31 ML, and a parabolic confining potential normal to the wires. For the analysis of broad strips, where several subbands are occupied, we referred to some previous results using the time-dependent local density approximation.[38,39] The quasi-1D fit shows very good agreement with the dispersion data as a function of $k_\parallel$ and demonstrates the 1D character of the plasmon dispersion. The one-dimensional electron concentration, N_{1D}, and the effective electron mass, m^*, are variable parameters for the plasmon dispersion. However, our local-field correction calculation has shown that the slope of the linear dispersion is determined only by the ratio N_{1D}/m^*.

Due to this strict scaling of the dispersion with N_{1D}/m^* for Pb/Si(111) at 1.31 ML coverage, m^* or N_{1D} cannot be determined directly from the plasmon dispersion curve. With the assumption of an effective mass of $0.4m_e$, which is the effective mass obtained from angle-resolved photoemission spectroscopy (ARPES) measurements,[25] we obtain an electron density $N_{1D} = 3.6 \times 10^7$ cm^{-1}. This density corresponds to a length of the Fermi wave vector along the wires of 0.57 Å^{-1} for a non-spin-polarized electron gas, which is about half of that found by ARPES measurements[25] under the assumption that the structural modulations along the wires, as found by LEED,[21] play no role for plasmon formation.

Because of the small width of the wires (1.55 nm), an electron system confined in the wire should be a 1D system where only a single subband is occupied. Actually, this 1D model explains the observed linear dispersion quite well. However, as stated above, this model leads to considerable underestimation of N_{1D}, and our system is at the borderline between 1D and 2D characters. In view of these facts, we suggest that 1D systems in neighboring wires get easily coupled to form a combined system where electron states extend in a strip region composed of adjacent wires. At 1.31 ML, at most, just a few wires are coupled to form a narrow-strip electron system where only a few subbands are occupied. This electron system retains 1D character, and the 1D model assuming an isolated strip can reproduce quite well the plasmon dispersion determined by the loss-peak position.

Let us briefly comment on the absence of plasmon excitation in the direction perpendicular to the wires. The average widths over a distribution of effective strip widths in the case described are much smaller than the wavelengths probed by our experiment in this direction. Therefore the probed electron has no substantial interaction with the induced charges. This explains why we detect no loss peak in this direction.

So far, we have analyzed the 1D character of the strip plasmons. The difference between 1D and 2D behavior is clearly seen by the comparison with high resolution electron energy loss spectroscopy (HREELS) data on flat Si(111), which we measured at the completion of the high-coverage $\sqrt{3} \times \sqrt{3}$R30° phase of Pb. The dispersion of this system, which turns out to be isotropic within the limits of uncertainty, is shown as squares in Fig. 4. The latter dispersion can be well fitted by the 2D calculation mentioned above. Including exchange-correlation effects, a wavelength independent screening by the Si substrate with dielectric constant $\epsilon_{Si} = 11.5$, and an effective electron mass in the Pb conduction bands of $m^* = 0.4m_e$, we obtain an effective electron concentration of $N_{2D} = 2.4 \times 10^{14}$ cm^{-2} participating in the plasmon formation. This concentration corresponds to approximately one electron per $\sqrt{3}$-unit cell. It indicates that the superstructure unit cell on the flat Si(111) surface is indeed relevant and only electrons in partially filled bands within this periodicity participate in plasmon formation.

Next, we turn our attention to the FWHMs that are large even at small $k_\parallel$ (see Fig. 5). If we stick to the above model assuming the isolated strip, the large FWHMs can only be

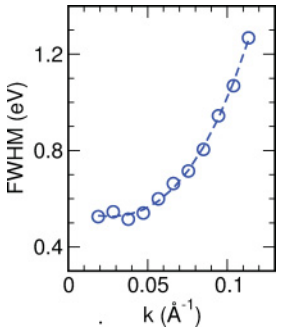

FIG. 5. (Color online) Changes of half-widths (FWHM) as a function of $k_\parallel$ for a Pb concentration of 1.31 ML. The dashed line is only a guide to the eye. Please note that for the Pb coverage of 1.31 ML only data along the step direction exist.

explained by strong damping. Even in the limit $k_\parallel \to 0$, the FWHM doesn't get smaller than 500 meV, as seen in Fig. 5. If the loss peaks in this limit consist of single peaks, the FWHM corresponds to plasmonic lifetimes of the order of 10^{-15} s. With the group velocity of 1.9×10^6 m/s determined from the slope of the dispersion at 1.31 ML of Pb, we obtain elastic mean-free paths, λ_{mfp}, of only 20 Å. This would mean that λ_{mfp} is generally shorter than the plasmonic wavelength, and a formation of a normal traveling wave is not possible, especially in the long-wavelength limit. This is unphysical and contradicts our results. Since the dispersion can clearly be measured down to $k_\parallel = 0.02$Å, λ_{mfp} must be larger than 300 Å.

The linewidth broadening of the plasmon, which remains large even in a small $k_\parallel$ range, could be ascribed to Coulomb interaction between adjoining metallic strips. In the absence of the interaction, the plasmon dispersions of the strips become degenerate or almost degenerate. However, switching on the interaction, removes this degeneracy, and gives rise to splitting of these dispersions (see Fig. 1 in Ref. 35). The interaction becomes stronger when $k_\parallel$ decreases. In the highest-energy mode, the induced-charge density distributions along these neighboring strips are coherent, and the dispersion of this mode is very close to that of the 2D plasmon. Since the energy of the higher-energy modes close to $k_\parallel = 0$ rises quickly from zero as a function of $k_\parallel$, the energy range of the split modes retain a finite and significant width, even at small $k_\parallel$. This dispersion splitting could account for the linewidth broadening that persists down to small $k_\parallel$ values.

B. Transitions between 1D and 2D: plasmons at other Pb concentrations

Data at other Pb concentrations than the one discussed above in the physical monolayer range at 1.2 and 1.4 ML were also taken. Contrary to the quasi-1D behavior at 1.31 ML, they are both characterized by the onset of a dispersing loss peak also in the direction normal to the steps, but at shorter wavelengths than in parallel direction. This means that we observe a transition from 1D to still anisotropic 2D properties. Sample spectra, comparing all three coverages, are shown in Fig. 6. Interestingly, we get significantly higher intensities at 1.2 and 1.4 ML than at 1.31 ML at the same $k_\parallel$ values, which indicates larger coherently scattering areas at the former two

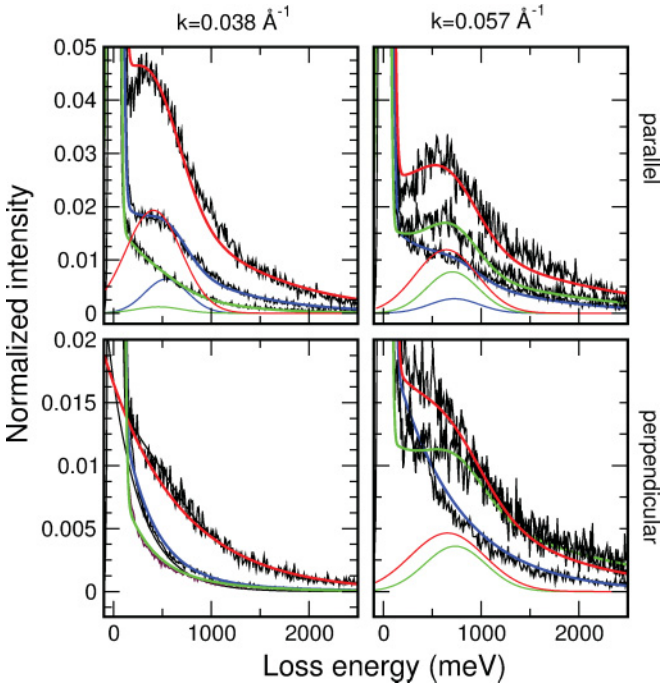

FIG. 6. (Color online) Selected loss spectra at Pb concentrations of 1.2 (green), 1.31 (blue), and 1.4 ML (red) parallel (top) and perpendicular to the step direction. Lines are fitted curves, the plasmonic loss is plotted separately at the bottom of each panel after background subtraction. Note that no plasmon loss can be identified at 1.31 ML in the direction normal to the steps.

coverages than at 1.31. ML. We assign this feature to the increased coupling strength between wires.

Comparing the dispersion curves obtained from the loss spectra at 1.2 and 1.4 ML Pb coverage (see Fig. 7), they qualitatively show a surprisingly similar behavior, namely, quasilinear dispersion both parallel and normal to the step direction, although with varying slope. Also the onset of a detectable signal, particularly in the direction normal to the steps, depends on the Pb concentration, i.e., on the Pb-induced structure, which is significantly different between

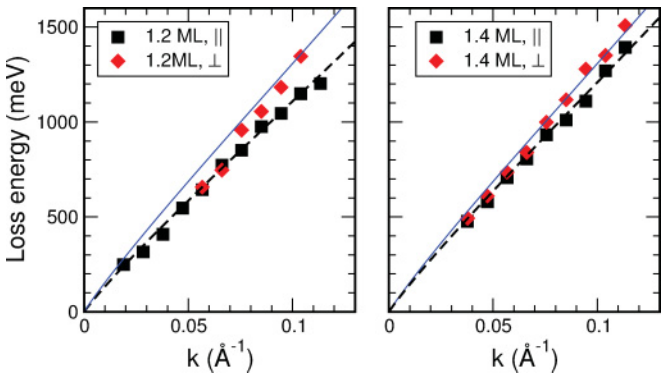

FIG. 7. (Color online) Dispersion parallel (■) and perpendicular (♦) to the step direction for Pb concentrations of 1.2 (left) and 1.4 ML. Dashed lines mark fits with the 1D model for the parallel direction (see text). The 1D results at 1.31 ML are plotted as a solid line for comparison.

1.2 and 1.4 ML (see below). Nevertheless, the existence of dispersing plasmonic losses normal to the step direction, though only at smaller wavelengths than parallel to the steps, means that a much larger number of Pb wires than at 1.31 ML must be coupled, and coupled so strongly that plasmonic wave propagation across the steps is easily possible.

Before we quantify the dispersions in more detail, we want to sketch ideas why coupling between Pb wires on the miniterraces may vary strongly with Pb concentration by briefly recalling some structural details at the various Pb concentrations obtained with LEED.[26] The 1.31 ML Pb layer consists of (223)-oriented minifacets in which the step edges are not covered by Pb. This apparently leads to the weak coupling described above, the small effective width of the wires and a small excitation probability because of the small electrical moments involved. By adding Pb to the 1.31 ML coverage, the step edges become decorated.[26] This decoration not only effectively reduces the band gap in the direction normal to the steps,[27] but also increases coupling between steps.

At 1.2 ML Pb coverage, not the (223) facets are stabilized, but the preferred facet orientation changes to (112), which coexists with (111)-oriented terraces in order to compensate for the higher slope of the (112) facets.[21] On the (111) terraces, Pb forms a $\sqrt{7} \times \sqrt{3}$ superstructure. From the spot size in LEED, we estimate an average terrace width of about 10 nm normal to the steps. Since there are no signs of step decoration by Pb, the majority of Pb atoms must be on the (111) terraces. The measured dispersion on this surface deviates significantly from the dispersion on the (111) surface (cf. with Fig. 4), but must be characteristic for these anisotropic Pb covered strips, most likely with some contributions from bundles of the (112) facets mixed in.

Based on these structural results, we now try to sketch a possible physical scenario that qualitatively explains the experimental findings, especially the quasilinear dispersion in both directions. This scenario is based on enhanced coupling between individual wires, which includes for the 1.2 ML coverage, the formation of a mixture of wires on (112) facets and small anisotropic (111)-oriented miniterraces. The decoration of step edges by Pb at 1.4 ML clearly acts toward stronger coupling of wires. This coupling then must allow formation of traveling waves across the strip at sufficiently short wavelengths in order to explain our results. However, the effective anisotropy of the strip must still be so pronounced as to maintain qualitatively the 1D character.

In fact, such a model has some justification, as seen by analyzing the dispersion data for the 1.2 ML coverage in more detail (see Fig. 7). We find that parallel to the steps, the dispersion can quantitatively be described by the lowest-energy mode in the 1D model of strips of finite width. The variation of the width between 3 and 10 nm does not change the 1D character of the curve, but essentially only rescales the electron density, in agreement with our model. In experiment, the slope of the dispersion is about 20% smaller than at 1.31 ML coverage. If we assume that electron density and effective electronic mass are essentially the same as for 1.31 ML, the reduction of slope is qualitatively described by our model.

Perpendicular to the steps, a plasmon loss signal was measurable only above $k_\perp$ values of 0.05 Å^{-1}, again with a quasilinear signature and a slope that is even higher by about 10% than in parallel direction. While we cannot easily explain the 1D signature, the onset of dispersion is compatible with our model: a strip width of 6 nm is required in order to form the lowest-energy mode of a standing wave of this wavelength. This width, therefore, sets a lower limit of effective widths in perpendicular direction, but more than twice this length is necessary for a traveling wave, which agrees well with the average strip width estimated from LEED. This small value underlines the high anisotropy of the Pb system at this concentration. At shorter wavelengths (larger k) traveling waves are possible also in $k_\perp$, but with a lifetime limited by the strip widths. This strong damping may also influence the measured dispersion and any deviation from quasilinear behavior, as, e.g., exhibited by the data points close to the onset of $k_\perp$ dispersion.

A similar picture holds for the data at 1.4 ML coverage. Here, a plasmonic loss signal can only be observed above $k = 0.035$ Å^{-1} in both directions, but again with the same quasilinear signature as just described for the 1.2 ML case and slopes slightly below that at 1.31 ML. This fits into a scenario where the increased electron density by the increase of Pb coverage from 1.2 to 1.4 ML is overcompensated by the generally larger effective widths of the investigated system, if we assume that all other parameters remain unchanged. Following the argumentation from above, the minimum k for an observable loss sets a limit for the definition of plasmonic traveling waves. Correlations are facilitated for shorter wavelengths, which involves a smaller number of terraces, in agreement with the observed quick increase of loss intensities (see Fig. 6) as a function of k after the onset of observable losses and the considerably higher intensities also parallel to the terraces compared with the 1.31 ML situation at all k values.

In all three cases investigated here, the plasmonic wavelengths are much longer than the width of individual miniterraces so that the atomistic details of the system should be of minor importance. Although we see a dispersion in 2D, it is important to note that anisotropy is still governing these systems. It obviously leads to two separate dispersion branches parallel and perpendicular to the miniterraces.

A qualitative, though still tentative, explanation for the linear plasmon dispersion in the perpendicular direction can indeed be given; when the probed wave vector is perpendicular to the strips, we observe those plasmon modes with $k_\parallel \approx 0$ where the induced charge density has a wavelike oscillation across the strip, but is almost constant along the strip. Each conduction electron feels the Coulomb potential generated by those induced charges that extend over a distance of the order of wavelength across the strip from the electron. This induced potential gives rise to the major part of the restoring force driving the induced-charge oscillation. The finite-width effect originates from the fact that the induced charges are missing outside the strip. When the probed wavelength across the strip is small compared with the strip width, the plasmon character is similar to that of the 2D plasmon. However, when this wavelength becomes comparable to or larger than the strip width, the restoring force driving the induced-charge

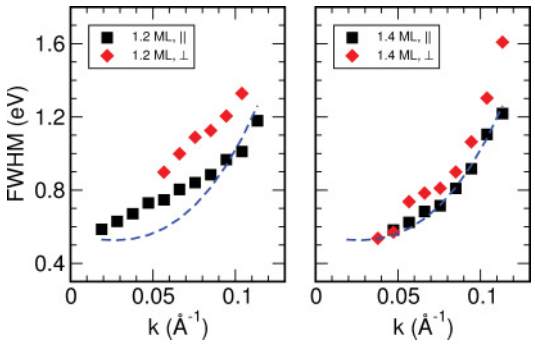

FIG. 8. (Color online) Full widths at half maximum of the plasmonic losses at 1.2 and 1.4 ML of Pb on Si(557) and for directions parallel (□) and perpendicular (◇) to the step direction. The FWHMs measured at 1.31 ML are indicated as dashed line for comparison.

oscillation does not operate so effectively as in the infinitely extended 2D system, which acts to lower the plasmon energy. This downward energy shift becomes larger as $k_\perp$ decreases, and could produce a linear dispersion rather than a dependence $\propto\sqrt{k_\perp}$.

As $k_\perp$ is varied, resonances occur only at those particular and discrete $k_\perp$ values, where the probed wavelengths match those of standing waves. However, since we found a distribution of strip widths, resonances happen at small $k_\perp$ intervals, which allow us to observe a well defined dispersion. This scenario also explains the vanishing loss intensity at small $k_\perp$, since in case of probed wavelengths, much larger than the strip width, the probe electron cannot interact with the induced charges effectively.

Looking finally at the widths of the plasmonic losses at Pb coverages of 1.2 and 1.4 ML, we find a similar dependence on k in both directions as for the 1.31 ML case and comparable widths. In particular, the FWHMs at 1.4 ML are almost the same as for 1.31 ML. This indicates that very similar mechanisms of broadening are effective at all coverages, i.e., the observed FWHMs at small k are not primarily determined by plasmonic lifetimes. From LEED, however, we know that the best ordered layers were obtained at 1.31 ML, but ordering even there was not perfect.

Therefore disorder, which shortens lifetimes of excitations, is again one of the possible broadening mechanisms. The 1.2 ML coverage has the highest FWHMs (see Fig. 8), but even there the differences to the FWHMs at the other Pb concentrations are less than 20% in $k_\parallel$ direction, so that disorder may not be the only mechanism contribution to the FWHM of plasmonic losses. Alternatively, linewidth broadening could arise again from the Coulomb interaction between neighboring wires similar to the 1.31 ML case. It becomes stronger with decreasing $k_\parallel$, and gives rise to splitting of the plasmon resonances. Thirdly, the slope of the dispersion on a strip of (fixed) finite width depends inversely on its width.[33] Therefore incoherent addition of contributions from strips of varying effective widths leads to FWHMs that increase continuously as a function of $k_\parallel$. For a linear dispersion and a fixed width, this addition will also lead to a linear increase of FWHMs. This may by the dominant contribution at large $k_\parallel$, while at small $k_\parallel$ additional subband splitting may contribute as a forth mechanism, as explained above.

This explanation of broadening mechanisms is reasonable for the direction parallel to the steps, but similar FHWMs and similar dependencies were also obtained to the direction normal to the steps. While plasmonic excitation lifetimes may finally become dominant at the highest measured k values, explaining the similarity of FWHMs for all systems for $k > 0.1$ Å^{-1}, more detailed structural investigations will be necessary in order to characterize the strip distributions under the various conditions so that more precise correlations between structure and plasmonic properties will be possible.

IV. SUMMARY AND CONCLUSIONS

The Pb/Si(557) system was already identified as being at the borderline between 1D and 2D behavior when structure and dc conductance have been investigated. This borderline is now extended to higher energy excitations in form of plasmons. We show here that various concentrations of Pb not only restructure the surface into a strongly anisotropic system, but they also have a strong influence on the coupling strength between the various terraces on the surface.

In all cases investigated here, i.e., close to but still below one physical monolayer of Pb, the investigated layers are governed by high anisotropy and a varying strength of coupling between the individual terraces on the surface. For the miniterraces of the (223) facets at 1.31 ML, the interterrace coupling of the conduction electrons is still so weak that in plasmonic excitations we find purely 1D properties at all k values accessible in our experiments. This correlates with the 1D behavior found in dc conductance at this Pb concentration. Broadening of the loss peaks in the limit $k_\parallel \to 0$, however, indicates that subband excitations are a possible characteristic for strip widths larger than one terrace.

Step decoration found at 1.4 ML obviously increases coupling between terraces to such an extent that now dispersion both parallel and perpendicular to the step direction was seen. While this marks at first sight the crossover from 1D to 2D, the measured dispersion curves remain characteristic of 1D behavior. This means that due to the high anisotropy, two separate plasmons exist in orthogonal directions with different group and phase velocities, which have 1D characteristics. This situation is similar at 1.2 ML Pb concentration but with modified interaction parameters and a larger degree of disorder in the system.

ACKNOWLEDGMENTS

T.I. acknowledges financial support from the Ministry of Education, Culture, Sports, Science, and Technology, Japan, Grand No. 22540332. He performed part of his numerical calculations at the Supercomputer center, Institute for Solid State Physics, University of Tokyo and Cyberscience Center, Tohoku University.

[1]T. Giamarchi, *Quantum Physics in One Dimension* (Oxford University Press, Oxford, 2004).
[2]G. Grüner, Rev. Mod. Phys. **60**, 1129 (1988).
[3]J. Voit, Rep. Prog. Phys. **58**, 977 (1995).
[4]J. Schäfer, C. Blumenstein, S. Meyer, M. Wisniewski, and R. Claessen, Phys Rev. Lett. **101**, 236802 (2008).
[5]C. Blumenstein, J. Schäfer, S. Mietke, S. Meyer, A. Dollinge1, M. Lochner, X. Y. Cui, L. Patthey, R. Matzdorf, and R. Claessen, Nat. Phys. **7**, 776 (2011).
[6]T. Kanagawa, R. Hobara, I. Matsuda, T. Tanikawa, A. Natori, and S. Hasegawa, Phys. Rev. Lett. **91**, 036805 (2003).
[7]J. N. Crain, A. Kirakosian, K. N. Altmann, C. Bromberger, S. C. Erwin, J. L. McChesney, J. L. Lin, and F. J. Himpsel, Phys. Rev. Lett. **90**, 176805 (2003).
[8]H. W. Yeom, S. Takeda, E. Rotenberg, I. Matsuda, K. Horikoshi, J. Schäfer, C. M. Lee, S. D. Kevan, T. Ohta, T. Nagao, and S. Hasegawa, Phys. Rev. Lett. **82**, 4898 (1999).
[9]J. R. Ahn, P. G. Kang, K. D. Ryang, and H. W. Yeom, Phys. Rev. Lett. **95**, 196402 (2005).
[10]T. Tanikawa, I. Matsuda, T. Kanagawa, and S. Hasegawa, Phys. Rev. Lett. **93**, 016801 (2004).
[11]C. Brun, I-Po Hong, F. Patthey, I. Yu. Sklyadneva, R. Heid, P. M. Echenique, K. P. Bohnen, E. V. Chulkov, and W. D. Schneider, Phys. Rev. Lett. **102**, 207002 (2009).
[12]I. Barke, F. Zheng, S. Bockenhauer, K. Sell, V. V. Oeynhausen, K. H. Meiwes-Broer, S. C. Erwin, and F. J. Himpsel, Phys. Rev. B **79**, 155301 (2009).
[13]S. V. Kravchenko and M. P. Sarachik, Rep. Prog. Phys. **67**, 1 (2004); R. E. Peierls, *Quantum Theory of Solids* (Clarendon, Oxford, 1955).
[14]S. Hasegawa, I. Shiraki, F. Tanabe, R. Hobara, T. Kanagawa, T. Tanikawa, I. Matsuda, C. L. Petersen, T. M. Hansen, P. Boggild, and F. Grey, Surf. Rev. Lett. **10**, 963 (2003).
[15]C. Tegenkamp, Z. Kallassy, H. Pfnür, H.-L. Günter, V. Zielasek, and M. Henzler, Phys. Rev. Lett. **95**, 176804 (2005).
[16]Ph. Hofmann and J. W. Wells, J. Phys. Condens. Matter **21**, 013003 (2009).
[17]F. Stern, Phys. Rev. Lett. **18**, 546 (1967).
[18]T. Nagao, S. Yaginuma, T. Inaoka, T. Sakura, and D. Jeon, J. Phys. Soc. Jpn. **76**, 114714 (2007).
[19]C. Tegenkamp, H. Pfnür, T. Langer, J. Baringhaus, and H. W. Schumacher, J. Phys. Condens. Matter **23**, 012001 (2011).
[20]H. Pfnür, T. Langer, J. Baringhaus, and C. Tegenkamp, J. Phys. Condens. Matter **23**, 112204 (2011).
[21]M. Czubanowski, A. Schuster, S. Akbari, H. Pfnür, and C. Tegenkamp, New J. Phys. **9**, 338 (2007).
[22]M. Czubanowski, A. Schuster, H. Pfnür, and C. Tegenkamp, Phys. Rev. B **77**, 174108 (2008).
[23]C. Tegenkamp, Z. Kallassy, H.-L. Günter, V. Zielasek, and H. Pfnür, Eur. Phys. B **43**, 557 (2005).
[24]H. Morikawa, K. S. Kim, D. Y. Jung, and H. W. Yeom, Phys. Rev. B **76**, 165406 (2007).
[25]C. Tegenkamp, T. Ohta, J. L. McChesney, H. Dil, E. Rotenberg, H. Pfnür, and K. Horn, Phys. Rev. Lett. **100**, 076802 (2008).
[26]M. Czubanowski, H. Pfnür, and C. Tegenkamp, Surf. Sci. **603**, L121 (2009).
[27]H. Pfnür, C. Tegenkamp, M. Czubanowski, D. Lükermann, J. Rönspies, and S. Wieß ell, Phys. Stat. Sol. B **247**, 2509 (2010).
[28]D. Lükermann, H. Pfnür, and C. Tegenkamp, Phys. Rev. B **82**, 045401 (2010).
[29]H. Claus, A. Büssenschütt, and M. Henzler, Rev. Sci. Instrum. **63**, 2195 (1992).
[30]M. Yakes, V. Yeh, M. Hupalo, and M. C. Tringides, Phys. Rev. B **69**, 224103 (2004).
[31]T. Nagao, T. Hildebrandt, M. Henzler, and S. Hasegawa, Phys. Rev. Lett. **86**, 5747 (2001).
[32]S. Das Sarma and W. Y. Lai, Phys. Rev. B **32**, 1401 (1985).
[33]E. P. Rugeramigabo, C. Tegenkamp, H. Pfnür, T. Inaoka, and T. Nagao, Phys. Rev. B **81**, 165407 (2010).
[34]W. I. Friesen and B. Bergersen, J. Phys. C **13**, 6627 (1980).
[35]T. Inaoka and T. Nagao, Mater. Trans., JIM **48**, 718 (2007).
[36]M. Jonson, J. Phys. C **9**, 3055 (1976).
[37]T. Inaoka, T. Nagao, S. Hasegawa, T. Hildebrandt, and M. Henzler, Phys. Rev. B **66**, 245320 (2002).
[38]T. Inaoka, J. Phys. Soc. Jpn. **73**, 2201 (2004).
[39]T. Inaoka, Phys. Rev. B **71**, 115305 (2005).